Successful Development of a 9.4T/800mm Whole-body MRI Superconducting Magnet at IEE CAS

Qiuliang Wang[1,2*], Yinming Dai[1], Hui Wang[1], Junsheng Cheng[1], Shunzhong Chen[1], Yaohui Wang[1], Hongyi Qu[1], Xinning Hu[1], Jianhua Liu[1], Chunyan Cui[1], Zili Zhang[1], Lei Wang[1], Hao Wang[1], Hui Liu[1], Jinshui Sun[1], Wanshuo Sun[1], Ling Xiong[1], Cong Wang[1], Dangui Wang[1]

[1] Division of Superconducting Magnet Science and Technology, Institute of Electrical Engineering, Chinese Academy of Sciences, Beijing 100190, China

[2]School of Electronic, Electrical and Communication Engineering, University of Chinese Academy of Sciences, Beijing 100049, China

* Corresponding author: Qiuliang Wang

Email: qiuliang@mail.iee.ac.cn

Abstract—The 9.4T whole-body MRI system is recognized as a powerful tool to explore the complex human bioinformatics and shows great application potential for the brain science research and early diagnosis of major neurodegenerative diseases. Due to the technical barrier of the 9.4T-level ultrahigh field superconducting magnet, only very few institutions in the world have the capability to apply the technology. Recently, the Institute of Electrical Engineering, Chinese Academy of Sciences (IEE CAS) successfully developed a 9.4T/800mm whole-body MRI superconducting magnet and the critical parameters all reach the project requirements. With the already prepared gradient assembly, RF assembly, and spectrometer console, the superconducting magnet will then go into the MRI system integration, which is arranged for the human metabolic imaging.

***Keywords (Index Terms)*—MRI, Superconducting magnet, Ultrahigh field, Metabolic imaging.**

1. Introduction

Since the first human image of a 9.4 T whole-body magnetic resonance imaging (MRI) system issued by the University of Minnesota in 2006 [1], the significant advantage of 9.4T-level human MRI has more strengthened people's confidence in MRI research towards ultrahigh magnetic field [2, 3]. With a strong magnet and gradient system, the 9.4T human MRI pushes the image resolution to a few hundred microns and even higher, which can observe the structure of human tissue in mesoscopic, providing more detailed physiological information to support structural pathological diagnosis and brain function analysis [4-6]. Moreover, the high signal-to-noise ratio of the ultrahigh magnetic field makes it feasible to image non-hydrogen elements with low abundance for the realization of multimodal imaging [7, 8]. For example, the elements Na^{23}, K^{39}, P^{31} and so on, are important components in human metabolites, and the tracking of these elements can provide critical metabolic information of the human body, which is potential to find a new therapy pathway for some complex diseases, such as Alzheimer's disease, Parkinson's Disease, and other neurodegenerative diseases [9, 10].

Up to the present, there are only several institutes in the world that have the capability to develop the 9.4T whole-body MRI techniques, for example, the University of Minnesota of the United States, Jülich Research Center of Germany, the Max Plank Institute of Germany, etc. Among the

systems, the most important hardware parts namely the main magnets, can be provided by very few professional companies, such as Tesla Engineering LTD Group. The extremely high technical difficulty of the ultrahigh-field large-bore superconducting magnet system has restricted the broad promotion of the 9.4T whole-body MRI [11].

At the end of October 2021, the Institute of Electrical Engineering, Chinese Academy of Sciences (IEE CAS) succeeded in exciting a 9.4T/800mm whole-body MRI superconducting magnet to the nominal magnetic field strength and then realized a persistent operation mode. The project started in 2011 to serve a major national science plan, which has gone through a nearly ten-year development period [12]. The self-developed superconducting magnet will be integrated into a complete MRI system to use for the metabolic imaging research.

2. Design and construction

The electromagnetic design pattern of the 9.4T/800mm MRI magnet adopts a compensating magnetic field optimization method to limit the peak magnetic field strength in the coils [13]. There are nine coils in total with five primary coils and four compensating coils. In addition, thirteen low-temperature shim coils were arranged outside the magnet coils, which include coils Z, X, Y, Z2, ZX, ZY, X2-Y2, XY, Z3, Z2X, Z2Y, Z(X2-Y2), ZXY. It requires about 5000L liquid helium to fill up the cryogenic container and there are four GM cryocoolers used to guarantee a zero helium-off. The cryogenic system design is shown in Fig. 1.

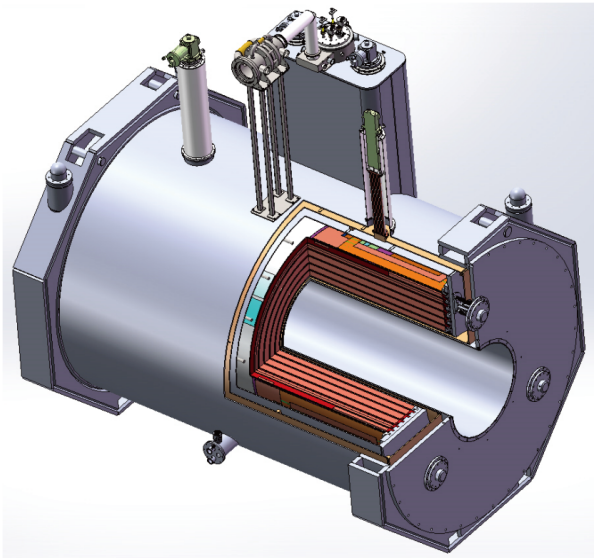

Fig. 1 Cryogenic system design of the 9.4T/800mm MRI superconducting magnet

Some typical fabrication process of the magnet is displayed in Fig. 2 [14, 15]. The completion of the magnet assembling was in 2018 and then a series of tests were conducted till the successful excitation.

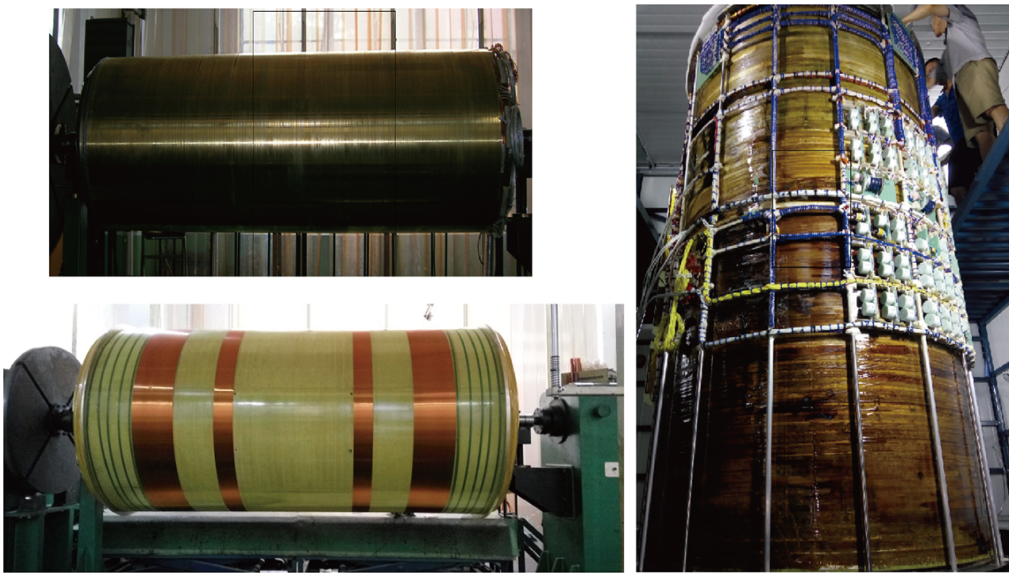

Fig. 2 Fabrication process of the 9.4T/800mm MRI superconducting magnet

3. Results and discussion

The acquired measurement parameters of the 9.4T/800mm MRI superconducting magnet are listed in Table I.

Table I Critical design parameters of the 9.4T/800mm MRI superconducting magnet

Central magnetic field strength	9.46T
Magnetic field stability	0.02ppm/h
Magnetic field homogeneity (without shimming)	74.91ppm (peak-peak)
Magnetic field homogeneity (with superconducting shimming)	15.82ppm (peak-peak)
Magnetic field homogeneity (with superconducting shimming and passive shimming)	0.28ppm* (peak-peak)
Cryogenic performance	Zero boiling off with four GM cryocoolers
Warm bore size	800mm
Magnet length	3662mm
Magnet weight	44.8t

*The passive shimming parameter is a simulated value.

Fig. 3 shows the magnetic field measurement using a Metrolab PT2025 NMR magnetometer. The 1062-8-10M probe has a measurement range of 6.0-13.7T and requires a magnetic field homogeneity of 50-120 ppm/cm. The meter display that the magnetic field strength at the magnet center is 9.4559T, which has a good agreement with our designed field-current efficiency.

Fig. 3 Magnetic field value measured by a Metrolab PT2025 NMR magnetometer

In order to test the magnetic field stability, we recorded the consecutive magnetic field data for three and a half days using the PT2025 NMR magnetometer. The magnetic field strength generally reflects a downtrend as shown in Fig. 4, although there are some fluctuations during the recording. Linear regression was applied to reveal the descending slope of the recorded data and it indicates a magnetic field decay rate of 0.02 ppm/h.

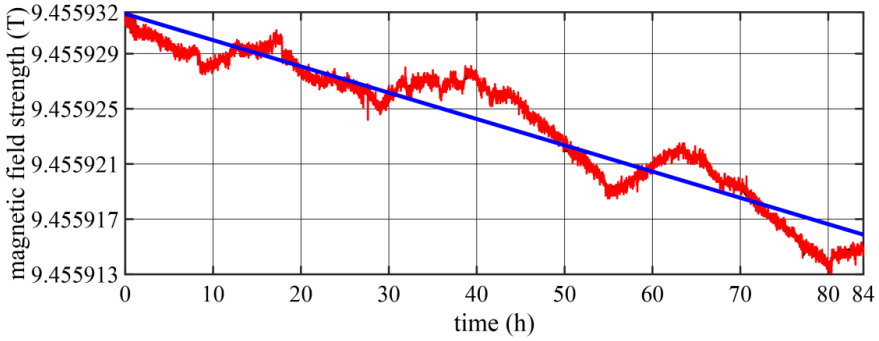

Fig. 4 Magnetic field stability for a consecutive duration

We also mapped the magnetic field distribution after the superconducting shimming operation over a 30cm sphere, which is illustrated in Fig. 5. The naked magnetic field homogeneity is

74.91ppm with peak to peak, that is 15.82ppm after superconducting shimming, and it is simulated to be 0.28ppm further with passive shimming.

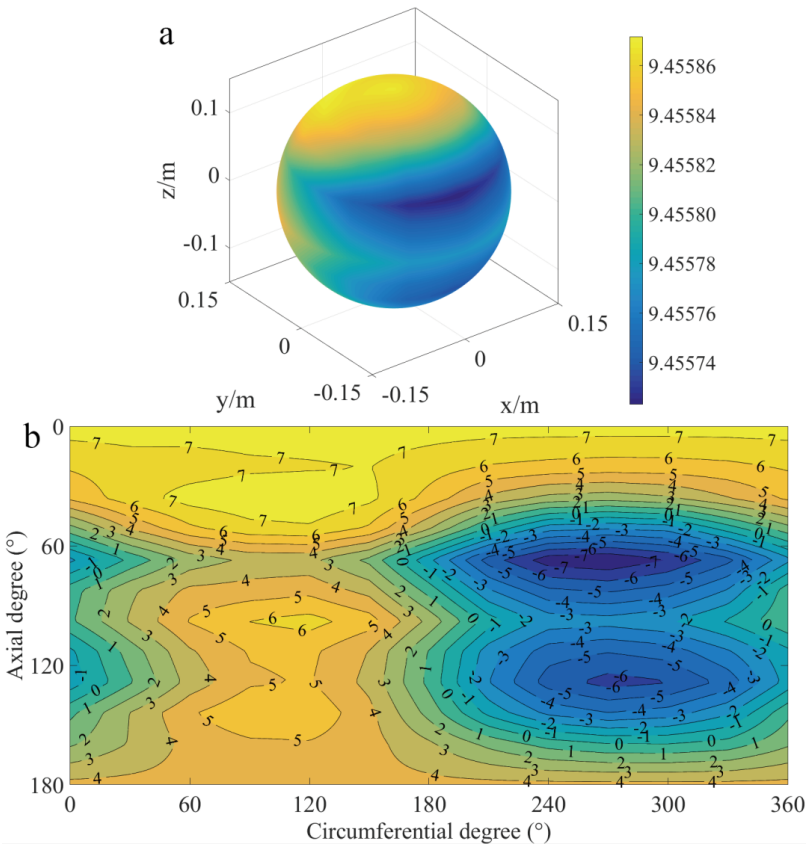

Fig. 5 Magnetic field distribution over a 30cm spherical volume: (a) magnetic field strength distribution (unit: T) and (b) magnetic field homogeneity distribution on the unwrapped spherical surface (unit: ppm)

The liquid helium consumption was observed by a high-precision liquid level meter. At the persistent mode, there is no obvious liquid level drawdown with one-week duration, which indicates a zero helium volatilization of the 9.4T/800mm MRI superconducting magnet system.

Since the target magnetic field strength has been achieved, we will go to shim the magnetic field for the next step, and then insert the self-developed gradient assembly and RF assembly. We hope to establish a complete MRI system to serve the brain science research program of China in the future.

4. Conclusion

A 9.4T whole-body MRI superconducting magnet has been developed successfully at IEE CAS and the core indices including the magnetic field strength, homogeneity, stability, cryogenic performance, fully meet the project requirements. The whole MRI system integration will be conducted afterwards.

Acknowledgements

This work was supported by the National Major Scientific Equipment R&D Project under Grant ZDYZ2010-2.

References

[1] T. Vaughan, L. DelaBarre, C. Snyder, J. Tian, C. Akgun, D. Shrivastava*, et al.*, "9.4T human MRI: Preliminary results," *Magnetic Resonance in Medicine,* vol. 56, pp. 1274-1282, 2006.

[2] E. Moser, "Ultra-high-field magnetic resonance: Why and when?," *World journal of radiology,* vol. 2, pp. 37-40, 2010.

[3] T. F. Budinger, M. D. Bird, L. Frydman, J. R. Long, T. H. Mareci, W. D. Rooney*, et al.*, "Toward 20 T magnetic resonance for human brain studies: opportunities for discovery and neuroscience rationale," *Magnetic Resonance Materials in Physics, Biology and Medicine,* vol. 29, pp. 617-639, 2016.

[4] O. Geldschläger, D. Bosch, N. I. Avdievich, and A. Henning, "Ultrahigh-resolution quantitative spinal cord MRI at 9.4T," *Magnetic Resonance in Medicine,* vol. 85, pp. 1013-1027, 2021.

[5] D. K. Deelchand, P.-F. V. d. Moortele, G. Adriany, I. Iltis, P. Andersen, J. P. Strupp*, et al.*, "In vivo 1H NMR spectroscopy of the human brain at 9.4T: Initial results," *Journal of Magnetic Resonance,* vol. 206, pp. 74-80, 2010.

[6] J. Budde, G. Shajan, K. Scheffler, and R. Pohmann, "Ultra-high resolution imaging of the human brain using acquisition-weighted imaging at 9.4T," *NeuroImage,* vol. 86, pp. 592-598, 2014.

[7] L. Ruhm, N. Avdievich, T. Ziegs, A. M. Nagel, H. M. De Feyter, R. A. de Graaf*, et al.*, "Deuterium metabolic imaging in the human brain at 9.4 Tesla with high spatial and temporal resolution," *NeuroImage,* vol. 244, p. 118639, 2021.

[8] N. J. Shah, "Multimodal neuroimaging in humans at 9.4 T: a technological breakthrough towards an advanced metabolic imaging scanner," *Brain Structure and Function,* vol. 220, pp. 1867-1884, 2015.

[9] G. Cattarinussi, G. Delvecchio, E. Maggioni, C. Bressi, and P. Brambilla, "Ultra-high field imaging in Major Depressive Disorder: a review of structural and functional studies," *Journal of Affective Disorders,* vol. 290, pp. 65-73, 2021.

[10] G. Donatelli, R. Ceravolo, D. Frosini, M. Tosetti, U. Bonuccelli, and M. Cosottini, "Present and Future of Ultra-High Field MRI in Neurodegenerative Disorders," *Current Neurology and Neuroscience Reports,* vol. 18, p. 31, 2018.

[11] R. Warner, "Ultra-high field magnets for whole-body MRI," *Superconductor Science and Technology,* vol. 29, p. 094006, 2016.

[12] Q. Wang, Y. Dai, B. Zhao, S. Song, C. Wang, L. Li*, et al.*, "A Superconducting Magnet System for Whole-Body Metabolism Imaging," *IEEE Transactions on Applied Superconductivity,* vol. 22, pp. 4400905-4400905, 2012.

[13] Y. Wang, Q. Wang, H. Wang, S. Chen, X. Hu, Y. Liu*, et al.*, "Actively-shielded ultrahigh field MRI/NMR superconducting magnet design," *Superconductor Science and Technology,* 2021.

[14] J. Cheng, L. Li, H. Wang, Y. Li, W. Sun, S. Chen*, et al.*, "Progress of the 9.4-T Whole-Body MRI Superconducting Coils Manufacturing," *IEEE Transactions on Applied Superconductivity,* vol. 28, pp. 1-5, 2018.

[15] Y. Dai, Q. Wang, C. Wang, L. Li, H. Wang, Z. Ni*, et al.*, "Structural Design of a 9.4 T Whole-Body MRI Superconducting Magnet," *IEEE Transactions on Applied Superconductivity,* vol. 22, pp. 4900404-4900404, 2012.